Received: August 20, 2023. Revised: October 30, 2023.

International Journal of
Intelligent Engineering & Systems

http://www.inass.org/

Enhancing Brain Tumor Detection and Classification with Reduced Complexity Spatial Fusion Convolutional Neural Networks

O. Homa Kesav[1] **Rajini G. K**[1]*

[1]*School of Electronics Engineering, Vellore Institute of Technology, Vellore, Tamilnadu, India*
* Corresponding author's Email: rajini.gk@vit.ac.in

Abstract: In this study, we propose a novel enhanced deep learning method for the detection and classification of brain tumours known as the reduced complexity spatial fusion CNN (RCSF-CNN) method. This approach integrates complexity feature extraction, which improves the quality of feature extraction from brain tumour pictures. To capture crucial detection properties, image variables such as mean, standard deviation, entropy, variance, smoothness, energy, contrast, and correlation are extracted. These attributes are then employed by the RCSF-CNN to detect and categorise brain cancers. When paired with the discrete orthogonal stockwell transform (DOST) as an intermediary stage, the suggested method illustrates the effectiveness and superiority of the augmented deep learning methodology for brain cancer identification. The studies were carried out using the BRATS dataset via Kaggle, with the network trained on 32 samples and the features of five sample pictures assessed. The RCSF-CNN stands out for its efficient architecture, which includes spatial fusion as well as a critical normalisation step. The addition of class activation mapping (CAM) increases transparency and interpretability, highlighting the model's innovation. The MATLAB simulation tool was used for implementation, and the experimental investigations were carried out on the free-source brain tumor image segmentation benchmark (BRATS) dataset. The results obtained in brain tumour identification reveal an entropy value of 0.008, an energy value of 0.8155, and a contrast value of 0.354. These entropy, contrast, and energy values are critical in the detection of brain tumors. Furthermore, in terms of accuracy, specificity, and sensitivity, the new technique beats earlier methods such as conventional CNN, deep learning with modified local binary patterns, and ML algorithms such as SVM in brain Tumour detection. The achieved accuracy of 98.99% indicates a high level of total correct classifications. The specificity of 99.76% illustrates the methodology's capacity to correctly identify non-tumor regions, while the sensitivity of 98.43% demonstrates its ability to correctly detect cancer locations.

Keywords: Brain tumor, Accuracy, Deep learning, CNN, Stockwell transform, Specificity, Sensitivity.

1. Introduction

Brain tumor is one of the most prevalent and devastating forms of cancer, accounting for a significant number of cancer-related deaths worldwide. Biopsy is an invasive procedure that carries some risks [1]. It involves the removal of a small sample of tissue from the body, which can cause bleeding, infection, or damage to surrounding structures. In some cases, the location of the tumor may make it difficult or impossible to obtain a biopsy sample. On the other hand, MRI is non-invasive procedure mostly utilized by the clinicians [2]. It can provide information about the size, location, and characteristics of a tumor. MRI is particularly useful for detecting brain tumors because it can detect even small tumors and can provide information about the tumor's location and relationship to other structures in the body [3]. MRI can also act as a repetitive process in order to evaluate the effectiveness of treatment [4] making MRI has become the mainstay.

Early detection and accurate classification of these cancers are critical for timely intervention and improved patient outcomes [5]. One of the major advancements in recent years is the use of deep learning techniques, particularly CNNs [6]. CNNs are capable of automatically learning hierarchical features, making them highly effective in detecting subtle patterns and features that may not be easily discernible by human observers [7-8]. Moreover,

deep learning models can be trained on large datasets, which has become increasingly available with the advancements in data collection and storage [9-10]. Our proposed methods' strengths include their ability to extract complex features from medical images using complexity feature extraction and GLCM. Furthermore, the use of CNNs enables automated and efficient analysis, allowing the detection of subtle and critical patterns. By incorporating the DOST as an intermediate stage, we improve the feature extraction process by capturing time-frequency characteristics of the input images. The availability of large-scale medical image datasets, as well as continuous advancements in deep learning techniques, provide an opportunity to develop robust models for accurate cancer detection. By leveraging these advancements and incorporating innovative techniques, our proposed methods aim to provide medical professionals with valuable tools for early and precise cancer diagnosis, ultimately improving patient care and outcomes.

The following is how the paper is organised: Section 1 contains the introduction, which provides an overview of the topic and highlights the strengths of the proposed work. Section 2 is divided into two sections: the first discusses the review of brain tumour detection methods, including previous methods and their limitations, emphasising the shortcomings of previous methods. Section 3 presents the improved methodology, which include block diagrams, algorithms, and the necessary equations for detecting brain tumours, section 4 is devoted to experimental investigations, which cover both subjective and objective evaluations, with extracted features tabulated in tables and graphs provided for greater comprehension. Section 5 summarises the key findings and contributions, suggests future research directions, and concludes with a references section listing the works cited.

2. Related works

Because of their potential to enhance early diagnosis and treatment results, image processing and deep learning approaches for detecting and classifying brain tumours have received a lot of interest. In this section, a analysis of the current literature on image processing and some of the latest deep learning techniques for the considered two specific applications is carried out.

The authors Lamrani et al. [11] proposed a CNN procedure for detecting brain tumours. Their work, however, did not address CNNs' limitations in handling complex spatial information and extracting fine-grained features, and statistically, this model provided good accuracy but a specificity of 75%, which is considered very low. Hasanah et al. developed a machine learning-based algorithm that used an SVM model as an intermediate stage [12]. While this method has potential, it is limited because of reduced accuracy of 82 % at Validation phase and also by its reliance on handcrafted features and may not capture the full complexity of brain tumour characteristics. Biratu et al. concentrated on the use of skull stripping and region growing procedures in the detection of brain tumours [13]. The accuracy achieved here is 99.7%, which is better, but the sensitivity is very low at 86.7%. The initial seed point selection is critical in determining the segmentation outcome. If the seed point is placed or chosen incorrectly, it can lead to significant errors in the segmentation results. This sensitivity is difficult to deal with, especially when dealing with complex or noisy images, because it necessitates careful manual intervention or human judgement to select appropriate seed points. While segmentation techniques can improve performance, this study did not investigate the capabilities of deep learning models in capturing intricate patterns and textures in brain tumour images. For feature extraction from brain MR scans, Kaplan et al. proposed using histogram patterns of local binary patterns (LBP) [14]. In image analysis, LBP is used as a texture descriptor. LBP takes texture into account only in local neighbourhoods and does not take into account spatial information between different local patterns. The spatial arrangement of textures in medical images can be critical for diagnosis. Although this method has proven to be effective, it may be lacking in the ability to capture high-level abstract features that are critical for accurate tumour detection. Abiwinanda et al. used a convolutional neural network (CNN) to classify tumours [15]. However, their approach is limited by the validation accuracy of 84 % and the lack of advanced feature extraction techniques and the possibility of overfitting due to the small dataset size. Malathi et al., [16] proposed brain tumour segmentation using convolutional neural network with tensor flow, with a low sensitivity of 82%, which is considered a significant limitation. This method makes many low-level decisions, which can be disadvantageous for high-level abstraction researchers. Nabil et al. [17] proposed a U-Net architecture for multimodal biomedical image segmentation with an accuracy of 91.65%, which is very low when compared to current scenarios. Amin et al. [21] proposed deep convolutional neural networks for brain tumour detection with a sensitivity of 95%, but they did not discuss validation accuracy well, which is a limitation of their work. The same

authors proposed brain tumour detection using statistical and machine learning methods [20], achieving 90% accuracy and specificity and 91% sensitivity, which is good but low when compared to current algorithms. Sharif et al [23-24] proposed two research articles: particle swarm optimisation (PSO) with feature fusion for brain tumour detection and active deep neural network features selection for segmentation and recognition of brain tumours using MRI images, where the researchers provided good results with better metrics. However, the performance of PSO is heavily dependent on parameter tuning, and the deep learning article provided a lower average accuracy of 92%. For the semantic segmentation of brain tumours from multimodal MRI scans, the authors, Ceena Mathews et al. [25], proposed a Nested U-Net architecture with an enhanced attention gate and compound loss. This method captures both low-level and high-level features effectively, improving segmentation precision and achieving sensitivity of 96.56%. However, the computational complexity of nested U-Net architectures, as well as potential computational efficiency issues, can be limiting factors.

Ahmed Aldhahab et al. [26] presented a framework based on stacked sparse autoencoders and a Softmax classifier for the classification of MRI brain tumour images with a 98.8% accuracy. While this method effectively performs image classification, it focuses on classification tasks and may necessitate a large amount of labelled data, which is often difficult to obtain in medical imaging.

The SDA-UNET2.5D, a shallow dilated with attention UNet2.5D architecture for brain tumour segmentation, was presented by the authors, Agus Subhan Akbar et al. [27]. This method provides a promising balance between depth and receptive field size, which may reduce computational requirements. However, there are some limitations, such as the emphasis on 2.5D MRI images and the lack of explicit discussions on computational efficiency. The authors also concentrated solely on dice score, with no comparison to sensitivity and specificity.

The authors, HPA Tjahyaningtijas et al. [28], proposed a brain tumour classification method with an accuracy of 95.5% using En-CNN (ensemble convolutional neural networks) applied to MRI images. While this method improves classification performance through ensemble methods, it is limited to classification and does not support tumour segmentation or localization. Furthermore, the computational cost of training and maintaining an ensemble of CNNs can be a limiting factor. The paper by Nyo MT et al. [20] adds to the growing body of literature on Otsu's thresholding technique's application in medical image analysis, specifically for brain tumour segmentation in MRI images. While Otsu's method is automated and simple, it has limitations in dealing with noise, multi-modal intensity distributions, and complex tumour boundaries.

Table 1 summarises brain tumour detection methods and their limitations. Traditional CNNs have good accuracy but low specificity. SVM validation accuracy is low and relies on handcrafted features. Region growing with skull stripping is sensitive in complex or noisy images. Local binary pattern (LBP) texture descriptors lack spatial information between local patterns. Validation accuracy limits a simple CNN architecture. CNNs with TensorFlow in Anaconda Frameworks have low sensitivity. Multimodal image-processing software MultiResUNet has low accuracy. Deep CNNs, which patch images, are sensitive but lack clarification on validation accuracy. Machine learning (ML) has good accuracy and specificity but lower sensitivity. Tuning parameters is difficult in integral particle swarm optimisation (PSO). Active DNNs have average accuracy. Nested U-Nets are computationally complex and inefficient. Though effective in classification, autoencoders may struggle with data labelling. SDA-UNET2.5D, for 2.5D MRI images, only discusses dice score and not computational efficiency. Finally, En-CNN and thresholding approaches strive to improve classification but not tumour segmentation or localization.

3. Proposed method

The proposed block diagram shown in Fig. 1, begins with obtaining the input image from a brain tumour database. The open source brain tumour image segmentation benchmark (BRATS) dataset [18] contains medical images of brain tumours. The proposed deep learning model was trained on an augmented dataset of 3000 samples generated from the BRATS dataset's initial 300 images [18]. To train the model to recognise complex tumour features, 80% of the augmented dataset, or 2400 samples, was used for training. The remaining 20%, totaling 600 samples, served as the test set, allowing the model's performance on data it had not encountered during training to be evaluated. After acquiring the input image, it is pre-processed with a Weiner filter. The Weiner filter is a type of linear filter used to reduce noise and enhance image features. This step produces a filtered image. After that, the filtered image is subjected to pixel normalisation and elimination. This procedure entails normalising the image's pixel

Table 1. A review on literature

Techniques Used	Mechanism	Limitations
CNN [11]	Traditional CNN procedure for detecting brain tumours.	this model provided good accuracy but a specificity of 75%, which is considered very low.
SVM [12]	a machine learning-based algorithm that used an SVM model as an intermediate stage	it is limited because of reduced accuracy of 82 % at Validation phase and also by its reliance on handcrafted features and may not capture the full complexity
Region Growing + Skull stripping [13]	The region growing algorithm either manually or semi-manually initialises the seed point, which influences the segmentation result.	sensitivity is very low at 86.7% and This sensitivity is difficult to deal with, especially when dealing with complex or noisy images
LBP [14]	LBP is used as a texture descriptor in Image Analysis	LBP only considers texture in local neighbourhoods, not spatial information between local patterns. Texture placement in medical images can aid diagnosis.
CNN [15]	Simple CNN architecture without any previous trained models has been used here.	approach is limited by the validation accuracy of 84 % and the lack of advanced feature extraction techniques
CNN + Tensor Flow [16]	Anaconda Frameworks were used by the Researchers.	a low sensitivity of 82%, which is considered a significant limitation.
MultiResUNet [17]	Used for multimodal images.	accuracy of 91.65%, which is very low when compared to current scenarios
Deep CNN [21]	They divided the image into multiple patches in pre-processing stage.	detection with a sensitivity of 95%, but they did not discuss validation accuracy well
ML [20]	Used statistical based Machine Learning	90% accuracy and specificity and 91% sensitivity, which is good but low when compared to current algorithms
Integral PSO [23]	PSO with feature fusion for brain tumour detection	PSO is heavily dependent on parameter tuning which can be a limitation
Active DNN [24]	deep neural network features selection for segmentation and recognition of brain tumours	lower average accuracy of 92%.
Nested U-Net [25]	Nested U-Net architecture with an Enhanced Attention Gate and Compound Loss.	Computational Complexity and Computational Efficiency are the limitations
Autoencoders [26]	While this method effectively performs image classification, it focuses on classification tasks	This method may necessitate a large amount of labelled data, which is often difficult to obtain in medical imaging.
SDA-UNET2.5D [27]	a shallow dilated with attention UNet2.5D architecture for brain tumour segmentation	emphasis on 2.5D MRI images and the lack of explicit discussions on computational efficiency. The authors also concentrated solely on dice score, with no comparison to Sensitivity and Specificity.
En-CNN [28]	improves classification performance through ensemble methods	it is limited to classification and does not support tumour segmentation or localization.
Otsu [29]	It is a Thresholding approach based on Classic Otsu method.	it has limitations in dealing with noise, multi-modal intensity distributions, and complex tumour boundaries.

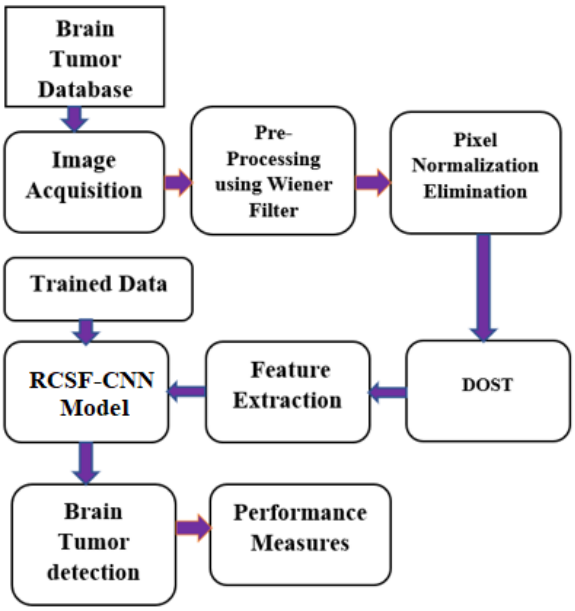

Figure. 1 Proposed brain tumor detection method

values to a standard range and removing any pixels that fall below a certain threshold value. This step produces a normalised and cleaned image. DOST is then fed the normalised and cleaned image. The DOST transform converts an image from the attained phase of the spatial domain to the corresponding value of the frequency domain. This aids in identifying the image's key features. DOST's output is then subjected to feature extraction. Identifying and extracting the image's important features is what feature extraction is all about. For tumour detection, the salient form of the features that have been extracted from the processed and transformed brain tumor images are fed to the CNN, which is considered as one of the finest and standard type of a deep neural network which is most often used for object recognition.

The algorithm described in this work aims to improve image quality and aid in the detection of brain tumors. The process begins with acquiring images from a medical database and applying a Wiener filtering procedure to pre-process the images. The pixel normalization elimination process is then initiated to normalize the pixels in the image. Next, the discrete orthogonal stockwell transform (DOST) is introduced as a transformation process to represent the image in the frequency domain. Features are then extracted using a complexity feature process. Finally, a RCSF-CNN process is applied, which is subtractive spatial light-weight-based, to detect brain tumors based on a trained dataset. The blocks in Fig. 1 are discussed briefly, and a description of the proposed deep learning approach with its novelty in technical terms is provided.

Pre-processing using weiner filter:

The Weiner filter is used in this approach to address the challenges posed by noise and artefacts in brain images, ultimately improving the quality and reliability of the images before further analysis. The Weiner filter is a critical step in the preprocessing pipeline, aiming to reduce noise while preserving important details in brain images.

Pixel normalization and elimination:

Pixel normalisation is the process of manipulating the pixel values of an image in order to enhance or remove certain features that disrupt the image's integrity. This section is also intended to normalise and fuse two input images using wavelet decomposition and the fusion methods specified. The function is flexible in terms of input arguments and output options, and it makes image normalisation and fusion operations simple.

Discrete orthogonal stockwell transform:

The discrete orthogonal stockwell transform is applied to the resulting image after the pixel normalisation and fusion steps. The DOST is a time-frequency representation that gives information about a signal's time and frequency components. The DOST coefficients represent the energy of the signal in various time and frequency domains. These coefficients can then be used as features in further analysis.

Feature extraction process:

The images are subjected to complexity-based feature extraction, which is based on a feature extraction process known as "Local Central Prominent." This method entails convolving an input image with a set of predefined filter kernels and then analysing the results to extract features that represent the image's local prominent patterns.

Reduced complexity spatial fusion CNN (RCSF-CNN) model :

The "Reduced Complexity Spatial Fusion CNN (RCSF-CNN)" method is a novel approach for accurately classifying brain tumours using medical images. The method is built around a lightweight CNN architecture that is strategically designed to reduce computational complexity while maintaining competitive performance. This efficiency is augmented by the incorporation of spatial fusion techniques, in which information from multiple sources, including potentially MR-based images, is combined using wavelet-based fusion. Notably, the method includes an important normalisation step that improves data fusion and interpretation. The model incorporates class activation mapping (CAM) to provide transparent insights into classification decisions, making it more understandable to medical

professionals. Its innovative use of lightweight design, spatial fusion, normalisation, and interpretability techniques. The approach's tailored design to address brain tumour classification challenges demonstrates its potential to yield accurate, efficient, and clinically meaningful results, advancing the field of medical imaging in healthcare applications.

The "Reduced Complexity Spatial Fusion CNN (RCSF-CNN)" introduces a significant innovation in accurately classifying brain tumours using medical images. The approach is built around a strategically designed lightweight CNN architecture that effectively balances computational efficiency with competitive performance. This efficiency is enhanced further by the incorporation of spatial fusion methodologies. Using wavelet-based fusion techniques, this fusion process combines information from various sources, including MR-based images. A notable addition is the inclusion of a critical normalisation step that improves data fusion quality and facilitates interpretation. The inclusion of class activation mapping (CAM) strengthens the model's explanatory power by providing medical professionals with transparent insights into classification rationale. The approach distinguishes itself through its unique combination of lightweight design, spatial fusion, normalisation, and interpretability techniques. Its personalised design aimed at addressing the complexities of brain tumour classification highlights its potential to generate precision, computational efficiency, and clinically significant outcomes.

Algorithm of reduced complexity spatial fusion CNN (RCSF-CNN)

Step i. Image acquisition from medical database and pre-process by means of Wiener filtering procedure.

$$F(u,v) = \frac{G(u,v)H(u,v)}{\left(|H(u,v)|^2 S(u,v) + N(u,v)\right)} \quad (1)$$

Where *F(u,v)* denotes the estimated image, *G(u,v)* depicts about the observed image, *H(u,v)* conveys the process of transfer function, *H*(u,v)* is referred as the complex conjugate values of *H(u,v)* function, *S(u,v)* denotes power spectral density, *N(u,v)* is considered as the PSD (power Spectrum) of the noise in the image.

Return the filtered image to the spatial domain. To obtain the filtered image in the spatial domain, use the inverse Fourier transform (IFFT). *P (i,j)* represents the pre-processed brain MRI scan using the Wiener filtering procedure.

Step ii. Initiate the pixel normalization elimination process

a. Calculate the mean value of pixel values in an image using the formula:

$$\mu = \left(\frac{1}{(M \times N)}\right) \Sigma\, P(i,j) \quad (2)$$

standard deviation :

$$\sigma^2 = \frac{1}{(M \times N)} \sum (P(i,j) - \mu)^2 \quad (3)$$

b. Normalize the pixel values in *P(i, j)* using the mean and standard deviation.

For each pixel *P(i, j)*, apply the normalization formula given by

$$P_{norm}(i,j) = \frac{(P(i,j) - \mu)}{\sigma} \quad (4)$$

The resulting image after pixel normalization is denoted as $P_{norm}(i,j)$ where each pixel value represents the normalized value of the corresponding pixel in the pre-processed brain MRI scan.

Step iii. Introduce the DOST as a Transformation process

a. calculate the corresponding DOST coefficient *C(t, f)* using the formula:

$$C(t,f) = \sum [P_{norm}(i,j)\, K(i - t, j - f)] \quad (5)$$

where:

Normalize the DOST coefficients and is given by

$$C_{norm}(t,f) = \frac{C(t,f)}{\sum |C(t',f')|} \quad (6)$$

Step iv. Extraction of features via complexity feature process

Step v. Involvement of CNN process which is reduced complexity spatial fusion CNN (RCSF-CNN) based to detect the brain tumors based on trained dataset.

4. Experimental investigations

The proposed deep learning model was trained on an augmented dataset of 3000 samples generated from the BRATS dataset's initial 300 images [18]. The aim was to improve the model's ability to detect brain tumours in medical images. By applying various transformations to the original images, data augmentation techniques expanded the dataset, enhancing the model's ability to recognise tumor-

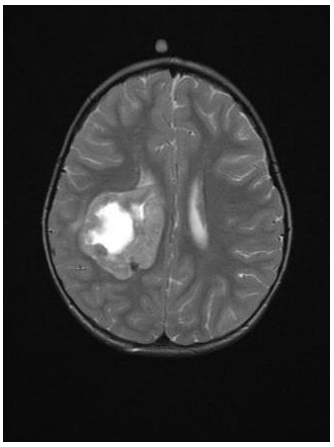

Figure. 3 Input brain scan

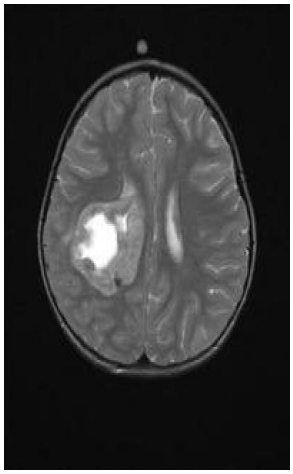

Figure. 4 Resized image

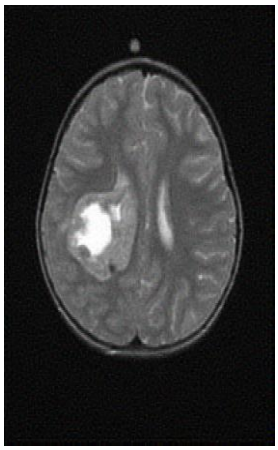

Figure. 5 Subtractive pixel extracted image

related patterns effectively. 80% of the augmented dataset (2400 samples) was used for training, allowing the model to recognise intricate tumour features. The remaining 20% (600 samples) comprised the test set, which evaluated the model's performance on previously unseen data. The input Brain scan, depicted in Fig. 3, is resized for optimal

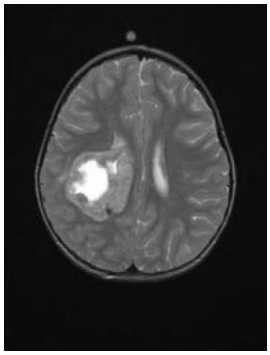

Figure. 6 Pre-processed image

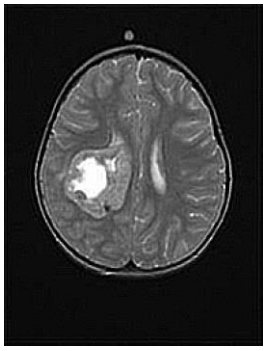

Figure. 7 Pixel noise ratio elimination

processing and depicted in Fig. 4, and its matching subtractive pixel extracted image, depicted in Fig. 5, is a critical component of the overall enhanced process.

Following that, Wiener filtering is used to remove any extraneous noise. The noise in the input image is analysed at this stage to determine its characteristics, such as the type of noise and the noise power spectrum. The PSD of the input image is estimated using an appropriate method that provides information about the image's frequency content. After that, the estimated PSD is used in the Wiener filtering algorithm to remove noise and improve the image. The Wiener filter is intended to minimise the mean square error between the filtered image and the original image while taking noise and signal characteristics into account. Finally, the filtered image is subjected to post-processing to remove any artefacts and improve the image's features. The final image in Fig. 6 shows the resultant images of the pre-processed image, and the pixel noise ratio has been reduced, as shown in Fig. 7.

After that, the stages that are involved in the extraction and elimination of subtractive spatial information. Next, the complexity feature extraction process is started. This process involves extracting the key image features such as mean, energy, contrast, and so on, which are essential in the detection process Fig. 8, and thus engaging RCSF-CNN to label the features. Afterwards, the detection process is

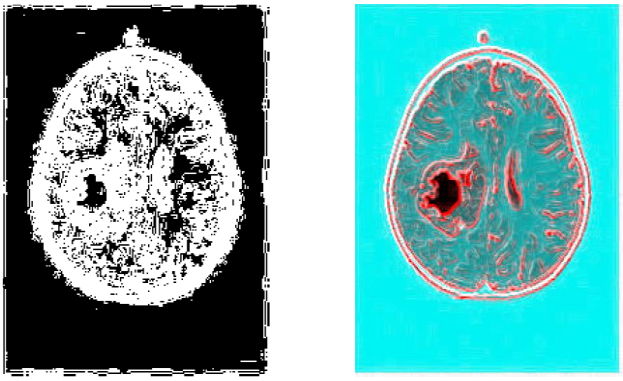

(a) (b)

Figure. 8 (a) & (b) Complexity feature extraction

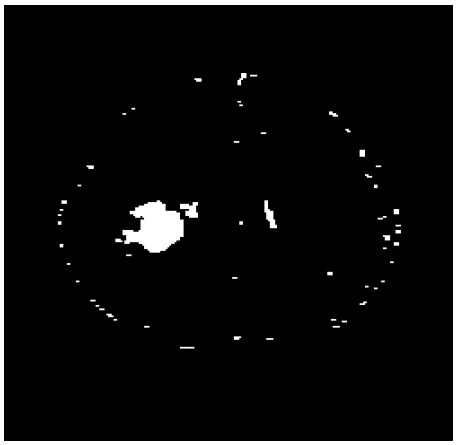

Figure. 9 Brain tumor detected area

completed.

When these extracted features are run through a RCSF-CNN and subjected to the trained dataset, the result is a brain tumour detection area, which, as Fig. 9 demonstrates, is an indication that a brain tumour has been found.

The proposed deep learning model underwent training on an augmented dataset comprising 3000 samples, which were generated from the original 300 images available in the BRATS dataset [18]. The primary objective was to equip this model with the ability to accurately detect brain tumors within medical images. Through data augmentation techniques, the initial dataset was expanded by applying diverse transformations to the original images, enhancing the model's capacity to generalize and identify tumor-related patterns effectively. Within this augmented dataset, 80% of the samples (2400 samples) were allocated for training, enabling the model to learn and internalize the intricate features associated with brain tumors. The remaining 20% (600 samples) were dedicated to the test set, evaluating the model's performance on unseen data. For feature extraction, the complexity technique was employed, involving the analysis of texture, spatial relationships, and other relevant attributes within the images. It's noteworthy that Table 2 presented a comprehensive summary of the features extracted from a subset of 5 samples, providing insights into the model's decision-making process for identifying brain tumors across the entire dataset.

The features that were extracted are provided with following equations:

Mean: The mean of an image is the average pixel value

$$\mu = \left(\frac{1}{N}\right)\sum_{i=1}^{n} I(i) \tag{7}$$

Here, N is considered as the over-all quantity of pixels in the image and *I(i)* denoted as the intensity value of the ith pixel.

Standard deviation: The standard deviation of an image is a measure of the amount of variation in the pixel values and is calculated as:

$$\sigma = \sqrt{\left(\left(\frac{1}{N}\right)\sum_{i=1}^{n}\ (I(i)-\mu)^2\right)} \tag{8}$$

Entropy: Entropy is a measure of the randomness or uncertainty in the pixel values of an image and is calculated as:

$$H = -\sum_{i=1}^{L} p(i) log2\big(p(i)\big) \tag{9}$$

L is denoted as the number of gray level values in the concerned image *p(i)* is considered as the normalized histogram of the image, and *log2* is known to be the base-2 logarithm.

Variance: Variance is a measure of how far the pixel values are from the mean and is calculated as:

$$\sigma^2 = \left(\frac{1}{N}\right)\sum_{i=1}^{n}(I(i)-\mu)^2 \tag{10}$$

Smoothness: Smoothness is a measure of how uniform the pixel values are and is calculated as:

$$S = \frac{1}{1+\sigma^2} \tag{11}$$

Contrast: Contrast is a measure of the difference between the pixel values in different regions of the image and is calculated as:

$$C = \frac{\mu_{max}-\mu_{min}}{\mu_{max}+\mu_{min}} \tag{12}$$

where μ_{max} and μ_{min} are the maximum and minimum pixel values in the image, respectively.

Correlation: Correlation is a measure of the

Table 2. Features extracted for samples of brain tumor images

	Sample Brain Tumor Images				
Features Extracted	**Sample 1**	**Sample 2**	**Sample 3**	**Sample 4**	**Sample 5**
Mean	0.0038	0.0046	0.00371	0.00432	0.0033
Standard Deviation	0.089	0.082	0.094	0.087	0.097
Entropy	0.0080	0.0074	0.0069	0.0076	0.0077
Variance	2.531	2.468	2.439	2.431	2.447
Smoothness	0.934	0.941	0.929	0.928	0.931
Contrast	0.354	0.347	0.348	0.366	0.358
Correlation	0.1067	0.1102	0.1123	0.1089	0.1094
Energy	0.8155	0.8321	0.8187	0.8167	0.8164

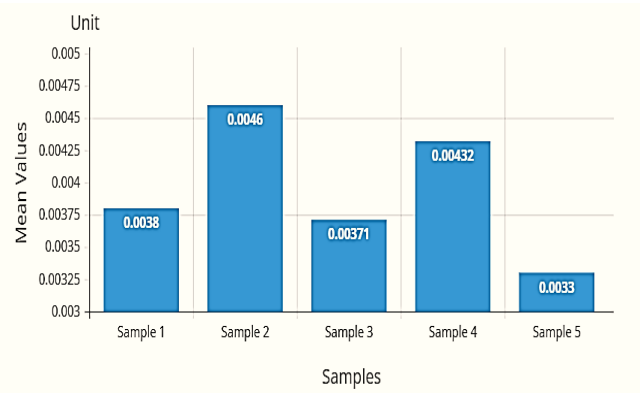

Figure. 10 Mean feature

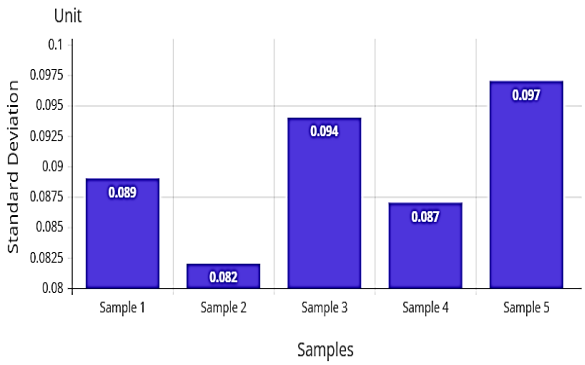

Figure. 11 Standard deviation feature

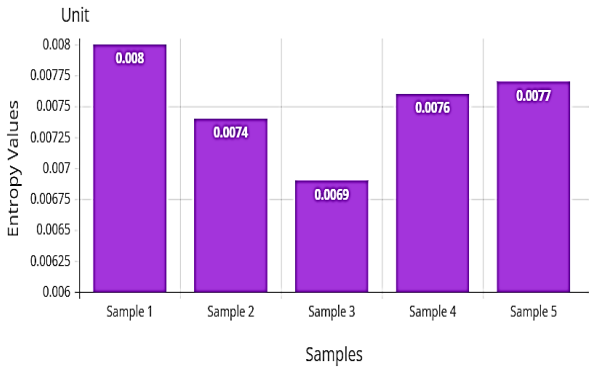

Figure. 12 Entropy feature

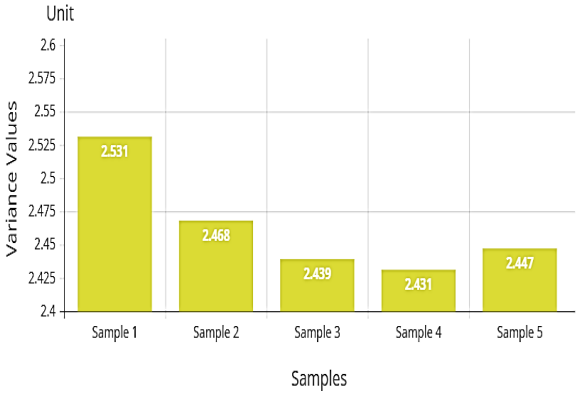

Figure. 13 Variance feature

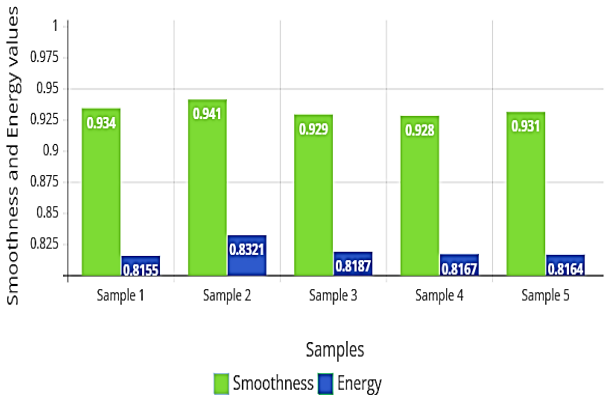

Figure. 14 Smoothness and energy features for brain tumor detection

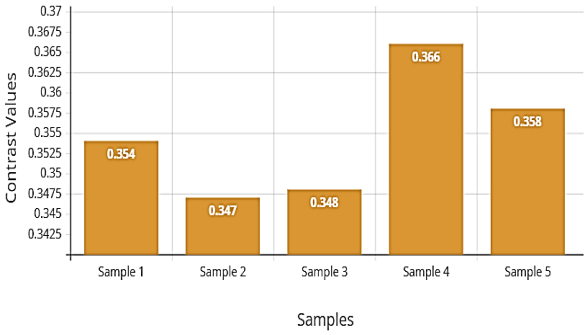

Figure. 15 Contrast feature

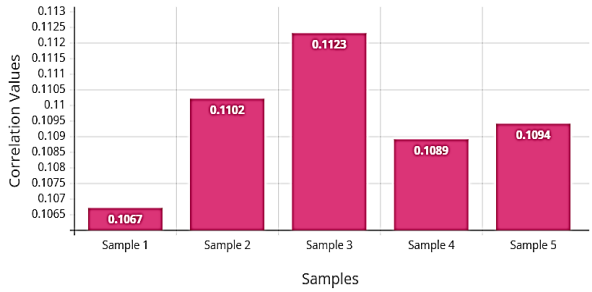

Figure. 16 Correlation feature

similarity between the pixel values in different regions of the image and is calculated as:

$$R = \frac{\left(\frac{1}{N}\right)\sum_{i=1}^{n}(I(i)-\mu_x)(J(i)-\mu_y)}{\sigma_x\sigma_y} \quad (13)$$

Energy: Energy is a measure of the total amount of energy in the image and is calculated as:

$$E = \sum_{i=1}^{n} I(i)^2 \quad (14)$$

The features which were tabulated are also represented in corresponding graphical plots where mean is drawn for 5 samples as shown Fig. 10, standard deviation in Fig. 11, entropy in Fig. 12, variance in Fig., 13, smoothness and energy in Fig. 14, contrast feature in Fig.15, and finally correlation in Fig 16 for the easy perception to see the behavior of features for each sample in the detection.

C. Performance evaluation

The BRATS-2015 dataset served as a common ground for comparing the proposed method to other existing methods in the context of the research being discussed. This ensures that the proposed method's evaluation and comparison are carried out under similar conditions and with the same dataset as the other methods. A standardised approach like this is critical in research because it allows for a fair and meaningful comparison of the effectiveness and performance of different algorithms. The BRATS-2015 dataset is a well-known and widely used dataset in medical image analysis, particularly for brain tumour segmentation and detection tasks. The BRATS-2015 dataset contains a diverse collection of brain magnetic resonance imaging (MRI) scans, including images of both normal brain tissue and tumor-affected brain regions. This dataset is thought to be useful for benchmarking and evaluating the performance of various algorithms and methods for brain tumour detection and segmentation.

In the context of brain tumour detection, accuracy is critical in determining the efficacy of developed methodology. A high accuracy value indicates that the proposed methods can correctly identify and classify tumour or cancer instances, whereas a low accuracy value indicates the presence of misclassifications or false predictions.

The accuracy of the brain tumor detection can be calculated using the following formula:

$$Accuracy = \frac{(TP + TN)}{(TP + TN + FP + FN)} \quad (15)$$

Here *TP* – true positive (identified Tumors),
TN – true negative, *FP* – false positive,
FN – false negative (not identified)

Specificity is the proportion of true negatives identified correctly by the model. It indicates the model's ability to correctly classify non-tumor or non-cancer cases.

$$Specificity = \frac{TN}{(TN + FP)} \quad (16)$$

Sensitivity is the proportion of true positives that were identified by the model. It indicates the model's ability to correctly classify tumour or cancer cases.

$$Sensitivity = \frac{TP}{TP + FN} \quad (17)$$

Table 3. Accuracy parametric comparison for brain tumor detection

Year	Techniques used	Accuracy (%)
2021	Enhanced Region Growing (ERG) [13]	98
2021	En-CNN [28]	95.5
2022	CNN [11]	96
2022	Thresholding [22]	95.559
	Proposed Method	**98.99**

Table 3 is a comparison table that shows the performance metrics of various methods for detecting brain tumours. The proposed methodology achieves 98.99% accuracy, 99.76% specificity, and 98.43% sensitivity. These metrics are compared to the findings of previous studies mentioned in the literature review.

Table 3 provides a comprehensive analysis of the accuracy of various brain tumour detection techniques conducted on the BRATS dataset. The method proposed in this study demonstrated a notable accuracy rate of 98.99%, surpassing the performance of all other recent studies listed in the table.

In general, the tabulated findings indicate that the proposed methodology has attained the highest level of accuracy, specifically 98.99%, when compared to other recent studies conducted on the BRATS dataset. This observation underscores the efficacy and pre-eminence of the proposed methodology in the identification of brain tumours compared to other cutting-edge techniques utilised in the same dataset. The superior accuracy achieved by the method proposed in this study suggests its potential to enhance performance and precision in the detection of brain tumours. This promising development contributes to the advancement of medical image analysis and the diagnosis of brain tumours.

Fig. 17 illustrates a graphical representation that allows for a visual comparison of the accuracy achieved by different brain tumour detection methods

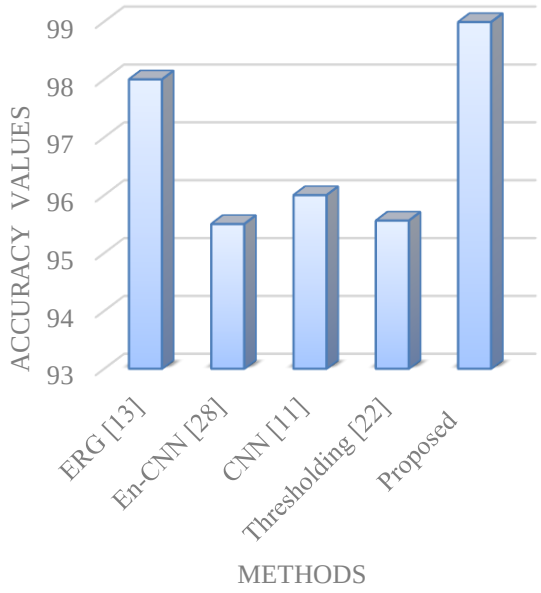

Figure. 17 Comparison plot for accuracy

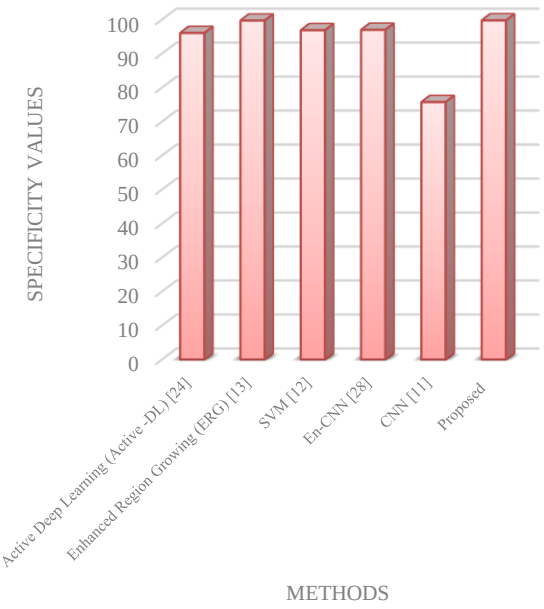

Figure. 18 Comparison plot for specificity

Table 4. Specificity parametric comparison for brain tumor detection

Year	Techniques used	Specificity (%)
2020	Active Deep Learning (Active -DL) [24]	96.06
2021	Enhanced Region Growing (ERG) [13]	99.7
2021	SVM [12]	96.87
2021	En-CNN [28]	96.97
2022	CNN [11]	75.72
	Proposed Method	**99.76**

when applied to the BRATS dataset. The plot demonstrates the efficacy of various methodologies, with the proposed approach exhibiting the highest level of accuracy at 98.99%. This exceptional performance distinguishes it as the most precise method when compared to other recent studies conducted on the BRATS dataset. The plot incorporates various additional methods which were reported in recent years The comparison plot provides clear evidence that the accuracy of the proposed method surpasses that of all other methods by a significant margin. The graphical depiction of accuracy values highlights the significant enhancement attained by the proposed methodology in the detection of brain tumours, as compared to the most advanced techniques employed on the BRATS dataset. The BRATS -2015 benchmark was used all the methods compared and also the proposed method also used similar data for a proper comparison. The increased level of accuracy attained by the method proposed in this study serves to strengthen its potential for enhanced precision and dependability in the detection of brain tumours. Consequently, it represents a promising and valuable addition to the domain of medical image analysis and the diagnosis of brain tumours. The utilisation of a comparison plot effectively presents a visually persuasive demonstration of the exceptional performance exhibited by the proposed method. This substantiates the method's efficacy in accurately detecting brain tumours and emphasises its significance in advancing the field of brain tumour diagnosis research.

The specificity values for different brain tumour detection methods, exclusively evaluated on the BRATS dataset, are comprehensively illustrated in Table 4. The specificity parameter quantifies the capacity of a methodology to accurately detect instances that are truly negative, a critical aspect in the prevention of false positive outcomes during the diagnosis of brain tumours. The table presents a compilation of various methodologies, including the proposed approach, as well as several recent studies. After careful examination of the table, it is apparent that the proposed method demonstrates a remarkable specificity of 99.76%. The exceptional level of specificity observed in this study demonstrates the considerable accuracy in correctly classifying healthy brain images as negatives, thereby reducing the likelihood of misdiagnosis or unnecessary interventions. Significantly, the specificity of the proposed method exceeds that of all other recent studies, thereby establishing its superiority in accurately discriminating between brain regions that

Table 5. Sensitivity parametric comparison for brain tumor detection

Year	Techniques used	Sensitivity (%)
2021	Enhanced Region Growing (ERG) [13]	86.7
2021	En-CNN [28]	97.03
2022	Thresholding [22]	68.79
2022	CNN [11]	95
2022	Nested U-Net [25]	96.56
	Proposed Method	**98.43**

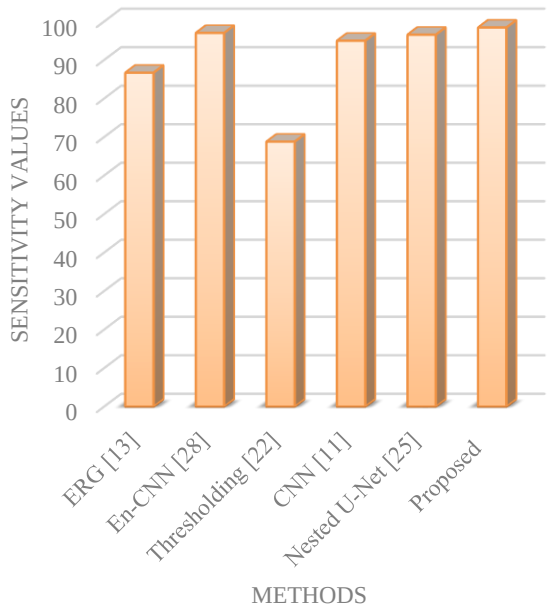

Figure. 19 Comparison plot for sensitivity

are healthy and those affected by tumours.

Fig. 18 depicts the comparison of specificity values for brain tumour detection methods on the BRATS dataset. The proposed method outperforms other recent works reported in literature in recent years. The visualisation of specificity values in Fig. 18 strengthens the proposed method's credibility and potential as a valuable tool in advancing medical image analysis for brain tumour detection.

Table 5 compares the sensitivity values for brain tumour detection methods on the BRATS dataset in detail. The proposed method's sensitivity of 98.43% outperforms other recent works that were tested on the same dataset. This high sensitivity value confirms the proposed method's accuracy in detecting tumor-affected regions, as well as its potential as a valuable tool in advancing medical image analysis for brain tumour detection. The findings in Table 5 demonstrate the proposed method's credibility and promise in contributing to the field of brain tumour detection and, ultimately, improving patient outcomes.

Fig. 19 depicts the sensitivity values for brain tumour detection methods using the BRATS dataset. The sensitivity of the proposed method is prominently displayed as the highest in the plot, clearly indicating its superiority over other recent works. This high sensitivity value reaffirms the proposed method's ability to detect brain tumours accurately, as well as its importance in contributing to improved patient care and medical decision-making in the field of neuroimaging.

5. Conclusion

To summarise, detecting and classifying brain tumours within medical images is a critical and intricate task. Image data's complexity and diversity frequently pose significant challenges to accurate analysis. In order to address this, we developed the reduced complexity spatial fusion CNN (RCSF-CNN), a novel approach that combines complexity feature extraction with a CNN-based detection and classification framework tailored for brain tumour identification. Notably, our model uses the discrete orthogonal stockwell transform (DOST) as an intermediate stage, which improves the robustness and precision of detection and classification processes. The effectiveness of our model has been demonstrated through extensive training and testing on a large dataset. We used 3000 samples, which were thoughtfully supplemented from the existing 300 images in the BRATS dataset [18]. This large dataset, which includes a wide range of brain tumour cases, underpins the model's dependability and versatility. 80% of the dataset was used for training, with the remaining 20% reserved for rigorous testing. It is worth noting that the proposed methodology achieved a remarkable accuracy rate of 98.99% for brain tumour detection, demonstrating its utility in real-world scenarios. This methodology emerges as a strong and dependable tool for the early detection and classification of brain tumours, resulting in improved therapeutic strategies and patient outcomes. Surprisingly, the high accuracy rates achieved highlight the efficacy of our proposed methodology across a wide range of cases. This study not only shows how our improved deep learning algorithm has the potential to revolutionise medical image processing, but it also emphasises the importance of a carefully curated and augmented dataset in improving model performance. Furthermore, the planned direction includes the development of user-friendly software or tools that incorporate these advanced deep learning techniques, making them

more accessible to healthcare professionals. By incorporating such tools into clinical workflows, they can play an important role in early brain tumour detection and classification, raising patient care and outcomes to new heights.

Notations list :

- Image pre-processing:
  - *I(i, j):* Pre-processed cancer image pixel at coordinates *(i, j)*
  - *L*: Number of possible intensity values (typically 256 for an 8-bit image)
- Histogram computation:
  - *h(k*): Number of pixels with intensity *'k'*
  - *MN*: Total number of pixels in the image
  - *cdf(k):* Cumulative distribution function of the histogram
- Intensity transformation:
  - *T(k):* Transformation function that maps intensity value k to its new value in the output image
- Segmentation:
  - *g(x, y*): Output image obtained by applying the transformation function to each pixel in the input image
  - *f(x, y):* Input image pixel at coordinates *(x, y)*
  - M, N: Dimensions of the image
- GLCM computation:
  - *G(i, j, dx, dy):* GLCM element at position *(i, j)* for displacement *(dx, dy)*
  - *I(m, n):* Pixel value at position *(m, n)* in the pre-processed image
  - *P (i, j, dx, dy*): Normalized GLCM element
- Texture features:
  - Contrast: Measure of difference between pixel values in different regions
  - Energy: Measure of total amount of energy in the image
  - Entropy: Measure of randomness or uncertainty in pixel values
  - Homogeneity: Measure of similarity between pixel values in different regions

Conflicts of interest

The authors affirm that they are aware of no personal or financial conflicts of interest that might have affected the research described in this paper.

Author contributions

O. Homa Kesav Conceptualization, Data curation Formal analysis, Methodology, Software Writing, original draft, investigation, resources.

Rajini G.K Writing—review and editing, visualization, supervision, project administration.

References

[1] T. A. Roberts, H. Hyare, G. Agliardi, B. Hipwell, A. D. Esposito, A. Ianus, J. O. B. Norris, R. Ramasawmy, V. Taylor, D. Atkinson, et al., "Noninvasive diffusion magnetic resonance imaging of brain tumor cell size for the early detection of therapeutic response", *Scientific Reports*, Vol. 10, 2020.

[2] J. E. V. Meyer, M. C. Mabray, and S. Cha, "Current Clinical Brain Tumor Imaging", *Neurosurgery*, Vol. 81, pp. 397–415, 2017.

[3] M. J. Rosenbloom and A. Pfefferbaum, "Magnetic Resonance Imaging of the Living Brain: Evidence for Brain Degeneration Among Alcoholics and Recovery With Abstinence", *Alcohol Research & Health: The Journal of the National Institute on Alcohol Abuse and Alcoholism*, Vol. 31, pp. 362–376, 2008.

[4] N. Lorenzovici, E. H. Dulf, T. Mocan, and L. Mocan, "Artificial Intelligence in Colorectal Cancer Diagnosis Using Clinical Data: Non-Invasive Approach", *Diagnostics*, Vol. 11, No. 3, p. 514, 2021.

[5] M. T. E. Melegy and H. M. Mokhtar, "Tumor Segmentation in Brain MRI Using a Fuzzy Approach with Class Center Priors", *EURASIP Journal on Image and Video Processing*, Vol. 2014, p. 21 pages, 2014.

[6] K. Munir, F. Frezza, and A. Rizzi, "Deep Learning for Brain Tumor Segmentation", *Studies in Computational Intelligence*, Vol. 908, pp. 189–201, 2021.

[7] S. Rajaraman, P. Ganesan, and S. Antani, "Deep Learning Model Calibration for Improving Performance in Class-Imbalanced Medical Image Classification Tasks", *PLoS ONE*, Vol. 17, p. e0262838, 2022.

[8] D. Selvaraj and R. Dhanasekaran, "MRI Brain Image Segmentation Techniques: A Review", *Indian Journal of Computer Science and Engineering*, Vol. 4, No. 5, pp. 364-381, 2013.

[9] J. G. Melekoodappattu, A. S. Dhas, B. K. Kandathil, and K. S. Adarsh, "Breast Cancer Detection in Mammogram: Combining Modified CNN and Texture Feature-Based

Approach", *Journal of Ambient Intelligence and Humanized Computing*, Vol. 2, pp. 1–10, 2022.

[10] I. Ahmed, Q. N. U. Rehman, G. Masood, and M. Nawaz, "Analysis of Brain MRI for Tumor Detection & Segmentation", In: *Proc of the World Congress on Engineering*, Vol. 1, p. 25, 2016.

[11] D. Lamrani, B. Cherradi, O. E. Gannour, M. Bouqentar, and L. Bahatti, "Brain Tumor Detection using MRI Images and Convolutional Neural Network", *International Journal of Advanced Computer Science and Applications*, Vol. 13, No. 5, pp. 45-59, 2022.

[12] U. Hasanah, R. Sigit, and T. Harsono, "Classification of brain tumor on magnetic resonance imaging using support vector machine", In: *Proc of the 2021 International Electronics Symposium (IES)*, Vienna, Austria, pp. 123-128, 2021.

[13] E. S. Biratu, F. Schwenker, T. G. Debelee, S. R. Kebede, W. G. Negera, and H. T. Molla, "Enhanced Region Growing for Brain Tumor MR Image Segmentation", *Journal of Imaging*, Vol. 7, No. 1, p. 22, 2021.

[14] K. Kaplan, Y. Kaya, M. Kuncan, and H. M. Ertunç, "Brain tumor classification using modified local binary patterns (LBP) feature extraction methods", *Medical Hypotheses*, Vol. 139, p. 109696, 2020.

[15] N. Abiwinanda, M. Hanif, S. T. Hesaputra, A. Handayani, and T. R. Mengko, "Brain Tumor Classification Using Convolutional Neural Network", In: *IFMBE Proceeding*, pp. 183–189, 2018.

[16] M. Malathi and P. Sinthia, "Brain Tumour Segmentation Using Convolutional Neural Network with Tensor Flow", *Asian Pacific Journal of Cancer Prevention*, Vol. 20, No. 7, pp. 2095-2101, 2019.

[17] I. Nabil and M. S. Rahman, "MultiRes UNet: Rethinking the U-Net Architecture for Multimodal Biomedical Image Segmentation", *Neural Networks*, Vol. 121, pp. 74-87, 2019.

[18] B. H. Menze, A. Jakab, S. Bauer, J. K. Cramer, K. Farahani, J. Kirby, Y. Burren, N. Porz, J. Slotboom, R. Wiest, L. Lanczi, E. Gerstner, M. A. Weber, T. Arbel, B. B. Avants, N. Ayache, P. Buendia, D. L. Collins, N. Cordier, J. J. Corso, A. Criminisi, T. Das, H. Delingette, Ç. Demiralp, C. R. Durst, M. Dojat, S. Doyle, J. Festa, F. Forbes, E. Geremia, B. Glocker, P. Golland, X. Guo, A. Hamamci, K. M. Iftekharuddin, R. Jena, N. M. John, E. Konukoglu, D. Lashkari, J. A. Mariz, R. Meier, S. Pereira, D. Precup, S. J. Price, T. R. Raviv, S. M. Reza, M. Ryan, D. Sarikaya, L. Schwartz, H. C. Shin, J. Shotton, C. A. Silva, N. Sousa, N. K. Subbanna, G. Szekely, T. J. Taylor, O. M. Thomas, N. J. Tustison, G. Unal, F. Vasseur, M. Wintermark, D. H. Ye, L. Zhao, B. Zhao, D. Zikic, M. Prastawa, M. Reyes, and K. Van Leemput, "The Multimodal Brain Tumor Image Segmentation Benchmark (BRATS)", *IEEE Transactions on Medical Imaging*, Vol. 34, No. 10, pp. 1993-2024, 2015, doi: 10.1109/TMI.2014.2377694. Epub 2014 Dec 4. PMID: 25494501; PMCID: PMC4833122.

[19] W. Deng, Q. Shi, M. Wang, B. Zheng, and N. Ning, "Deep Learning-Based HCNN and CRF-RRNN Model for Brain Tumor Segmentation", *IEEE Access*, Vol. 8, pp. 26665-26675, 2020.

[20] J. Amin, M. Sharif, M. Raza, T. Saba, and M. A. Anjum, "Brain Tumor Detection using Statistical and Machine Learning Methods", *Computer Methods and Programs in Biomedicine*, Vol. 177, pp. 69-79, 2019.

[21] J. Amin, M. Sharif, M. Yasmin, and S. L. Fernandes, "Big Data Analysis for Brain Tumor Detection: Deep Convolutional Neural Networks", *Future Generation Computer Systems*, Vol. 87, pp. 290-297, 2018.

[22] S. Nema, A. Dudhane, S. Murala, and S. Naidu, "RescueNet: An Unpaired GAN for Brain Tumor Segmentation", *Biomedical Signal Processing and Control*, Vol. 55, p. 101641, 2020.

[23] M. Sharif, J. Amin, M. Raza, M. Yasmin, and S. C. Satapathy, "An Integrated Design of Particle Swarm Optimization (PSO) with Fusion of Features for Detection of Brain Tumor", *Pattern Recognition Letters*, Vol. 129, pp. 150-157, 2020.

[24] M. Sharif, J. P. Li, M. A. Khan, and M. A. Saleem, "Active Deep Neural Network Features Selection for Segmentation and Recognition of Brain Tumors using MRI Images", *Pattern Recognition Letters*, Vol. 129, pp. 181-189, 2020.

[25] C. Mathews and A. Mohamed, "Nested U-Net with Enhanced Attention Gate and Compound Loss for Semantic Segmentation of Brain Tumor from Multimodal MRI", *International Journal of Intelligent Engineering and Systems*, Vol. 15, No. 4, 2022, doi: 10.22266/ijies2022.0831.23.

[26] A. A. S. Ibrahim and W. B. Mikhael, "Stacked Sparse Autoencoder and Softmax Classifier Framework to Classify MRI of Brain Tumor Images", *International Journal of Intelligent Engineering and Systems*, Vol. 13, No. 3, 2020, doi: 10.22266/ijies2020.0630.25.

[27] A. S. Akbar, C. Fatichah, and N. Suciati, "SDA-UNET2.5D: Shallow Dilated with Attention Unet2.5D for Brain Tumor Segmentation", *International Journal of Intelligent Engineering and Systems*, Vol. 15, No. 2, 2022, doi: 10.22266/ijies2022.0430.14.

[28] H. P. A. Tjahyaningtijas, D. J. Rumala, C. V. Angkoso, N. Z. Fanani, J. Santoso, A. D. Sensusiati, P. M. A. V. Ooijen, I. K. E. Purnama, and M. H. Purnomo, "Brain Tumor Classification in MRI Images Using En-CNN", *International Journal of Intelligent Engineering and Systems*, Vol. 14, No. 4, 2021, doi: 10.22266/ijies2021.0831.38.

[29] M. T. Nyo, F. M. Oudina, S. S. Hlaing, and N. A. Khan, "Otsu's Thresholding Technique for MRI Image Brain Tumor Segmentation", *Multimedia Tools and Applications*, Vol. 81, No. 30, pp. 43837-43849, 2022, doi: 10.1007/s11042-022-13215-1.